Journal of Molecular Liquids 351 (2022) 118614

Contents lists available at ScienceDirect

Journal of Molecular Liquids

journal homepage: www.elsevier.com/locate/molliq

Albumin-hyaluronic acid colloidal nanocarriers: Effect of human and bovine serum albumin for intestinal ibuprofen release enhancement

Alexandra N. Kovács [a], Gábor Katona [b], Ádám Juhász [a,c], György T. Balogh [d,e,*], Edit Csapó [a,c,*]

[a] MTA-SZTE Lendület "Momentum" Noble Metal Nanostructures Research Group, Interdisciplinary Excellence Center, Department of Physical Chemistry and Materials Science, University of Szeged, H-6720 Rerrich B. square 1, Szeged, Hungary
[b] Institute of Pharmaceutical Technology and Regulatory Affairs, Faculty of Pharmacy, University of Szeged, H-6720 Eötvös Str. 6, Szeged, Hungary
[c] MTA-SZTE Biomimetic Systems Research Group, Department of Medical Chemistry, Faculty of Medicine, University of Szeged, H-6720 Dóm square 8, Szeged, Hungary
[d] Institute of Pharmacodynamics and Biopharmacy, Faculty of Pharmacy, University of Szeged, H-6720 Eötvös Str. 6, Szeged, Hungary
[e] Department of Chemical and Environmental Process Engineering, Budapest University of Technology and Economics, H-1111 Műegyetem Quay 3, Budapest, Hungary

ARTICLE INFO

Article history:
Received 1 December 2021
Revised 18 January 2022
Accepted 24 January 2022
Available online 29 January 2022

Keywords:
Hyaluronic acid
Serum albumins
Biocolloids
Ibuprofen
Intestinal-PAMPA

ABSTRACT

Effective applicability of serum albumin-hyaluronic acid (HyA) conjugates as potential drug delivery colloidal particles having d ~ 220 – 260 nm average size has been presented for encapsulation of ibuprofen (IBU). Increased IBU content with drug loading of 30 % can be achieved via combination of the serum albumin proteins with biodegradable HyA polysaccharide. After optimization of the synthesis protocols and the characterization of the prepared systems for both bovine (BSA) and human serum albumin (HSA)-based particles, *in vitro* dissolution and intestinal-specific permeability studies were also performed. It was established that these protein/polysaccharide colloidal carriers have more favourable dissolution, intestinal permeability, and flux features than the unformulated IBU which is greatly controlled by the net charge of serum albumins at pH = 6.50. The nanosized carrier formula, which provides enhanced solubility, accelerated dissolution, and greater permeability, may represent a more controlled, lower dose loading, and gastric mucosa-sparing therapeutic solution in the high-dose IBU therapy.

1. Introduction

The improvement of novel drug delivery systems (DDSs) is of prime interest for the design of novel therapeutic approaches [1]. Due to their biocompatibility and biodegradability the natural polysaccharides are widely applied [2–4] in pharmacy; the extreme hydrophilic hyaluronic acid (HyA) is a natural linear glycosaminoglycan affected in different biological processes including cell growth or migration [5]. The role of serum albumins in the development of protein-based delivery systems is well-known [6] owing to the unique ability of binding features [7] as wide range of organic and inorganic compound can bind to the active region of the protein [8]. The strength of the interaction between protein and drug can be significantly affected via electrostatic interactions [9] by the change in the net charge of the macromolecule in the function of the pH [8], but the hydrophobic interactions are also decisive in some cases [10].

Protein-polysaccharide conjugates represent a novel candidate of possible drug carrier systems combining the beneficial properties of these macromolecules [11–14]. In our previous work [15], the bovine serum albumin (BSA)-HyA complex drug delivery system was prepared by a simple, one-step charge compensation method without the use of toxic and hardly removable crosslinking agents [16], surfactants, or organic solvents. In the combination of these macromolecules, the primary goal was to consider their solubility and net charge under the preparation conditions (pH = 4.5 acetate buffer). Several other combinations of protein – polysaccharide (*e.g.* casein- chitosan) systems do not meet these strict requirements. For the mentioned previous article [15], mainly the pH-dependent relationship between the macromolecules and the characteristic features of the prepared drug containing and drug - free colloidal conjugates are studied in detail, but several important aspects (*e.g. in vitro* dissolution, permeability *etc.*) were not published.

Non-steroidal anti-inflammatory drugs (NSAIDs) are widely applied to reduce pain, inflammation, body temperature in case

* Corresponding authors at: Institute of Pharmacodynamics and Biopharmacy, Faculty of Pharmacy, University of Szeged, H-6720 Eötvös Str. 6, Szeged, Hungary (G.T. Balogh) and MTA-SZTE Lendület "Momentum" Noble Metal Nanostructures Research Group, Interdisciplinary Excellence Center, Department of Physical Chemistry and Materials Science, University of Szeged, H-6720 Rerrich B. square 1, Szeged, Hungary (E. Csapó).

E-mail addresses: balogh.gyorgy.tibor@szte.hu (G.T. Balogh), juhaszne.csapo.edit@med.u-szeged.hu (E. Csapó).

https://doi.org/10.1016/j.molliq.2022.118614
0167-7322/

of fever, moreover they can be successfully applied therapeutically in rheumatoid arthritis, and moderate-to-severe osteoarthritis [17]. Oral administration of NSAIDs tend to cause serious gastrointestinal issues [18], ulcers and bleeding can be mentioned among the major side effects of the NSAIDs, therefore the chronic use of these agents in elderly and haemorrhagic patients is recommended only with extreme caution [19]. Ibuprofen (IBU) is known as one of the most frequently used NSAID compound [20], the mechanism of the action is based on by the inhibition of cyclooxygenase enzymes activity, which are responsible for the production of prostaglandins that reduces stomach acid and increases mucus production [21]. Due to the weak acidic character of IBU ($pK_a \sim 4.4 - 4.9$) [22] the intestinal dissolution rate strongly depends on the luminal pH and on the available small bowel volume limiting drug absorption. Therefore, our study aims to focus on to develop such carriers, which can increase intestinal dissolution rate and facilitate the intestinal absorption of IBU, thereby reducing the risk of adverse effects. In the scientific literature, the solubility and the bioavailability of the IBU were increased by Poloxamer 407 [23], polyethylene glycol 2000 [24], polyethylene glycol 8000 [25,26], and soy protein [27]. Albumin is a suitable choice for that purpose, as it can improve the solubility of drug, moreover they can bind and absorbed through the neonatal Fc receptor (FcRn), which is in large numbers expressed in the intestines [28].

As a continuation of our previous work, the optimization of IBU content of BSA/HyA complex carrier system was investigated in detail [15]. Besides the preparation of BSA-based particles, as a new system, the HSA-based colloidal carriers were also fabricated with increased drug content. To justify a promising pharmaceutical application the *in vitro* dissolution and intestinal-specific permeability studies are also performed. The drug release from the complex carriers and the species-specific protein-drug interaction has also been extensively studied. The application of this complex DDS can imply a novel alternative for the controlled release of NSAID compounds that may reduce the occurrence of adverse side effects.

2. Materials and methods

2.1. Materials

Human serum albumin (HSA; ~ 67 kDa) was purchased from Serva Electrophoresis GmbH. Bovine serum albumin (BSA; ~ 66 kDa), the hyaluronic acid sodium salt (HyA; 1.5 – $1.8 \cdot 10^3$ kDa), ibuprofen sodium salt (IBU; ≥ 98%), phosphate buffered saline (PBS) powder, disodium hydrogen phosphate (Na_2HPO_4), sodium dihydrogen phosphate (NaH_2PO_4), L-α-phosphatidylcholine (PC) and cholesterol (CHO) were obtained from Sigma-Aldrich. The sodium acetate 3-hydrate ($CH_3COONa \cdot 3H_2O$; ≥ 99%), and sodium hydroxide (NaOH; ≥ 96%) pastilles, the hydrochloric acid (HCl; ≥ 99%), and the acetic acid (AcOH; ≥ 99%) were bought from Molar Chemicals. Analytical grade solvents such as acetonitrile (MeCN), dimethyl sulfoxide (DMSO) and dodecane were purchased from Merck KGaA (Darmstadt, Germany). Highly purified water was obtained by deionisation and filtration with a Millipore purification apparatus (18.2 MΩ·cm at 25 ℃). All reagents/solvents were used without further purification.

2.2. Preparation of drug-free BSA/HyA and HSA/HyA nanocarriers

The protein/polysaccharide complex colloidal particles are prepared with a slight modification [15]. The optimal mass ratio of the macromolecules was obtained at $m_{BSA}:m_{HyA} = 2:1$. Firstly, the HyA stock solution (0.2 mg mL^{-1}; 10 mL) was prepared in acetate buffer (0.010 M acetic acid/0.0057 M sodium-acetate; pH = 4.5) and stirred at 370 rpm for 60 min and stored at least 12 h (5 °C). Secondly, BSA and HSA were dissolved in highly purified MilliQ water (2 mg mL^{-1}; 2 mL), separately and stirred for 30 min. For preparation of the complex particles, the BSA or HSA solutions were added drop-by-drop to the HyA solution and stirred for 1 h using 370 rpm. Upon addition of HyA, the initial colorless solution turned into a slightly opalescent colloidal dispersion indicating the formation of nanosized particles as the inserted photo in Fig. 2. presents. For purification, the samples were centrifugated at 15,000 rpm for 30 min, the supernatant was removed, and the samples were redispersed in acetate buffer (pH = 4.5) solution. After purification, the samples were freeze-dried, and the lyophilized powders were stored in −70 °C.

2.3. Preparation of IBU-loaded BSA/HyA and HSA/HyA colloidal particles

The IBU-loaded carriers were prepared in the same way as the unloaded systems [15]. For optimization of IBU-content, appropriate amounts of IBU (m_{IBU}/m_{BSA} = 0.125 – 4.0 (0.50 mg – 16.0 mg IBU/4.0 mg BSA)) were dissolved in the protein-containing solutions. The protein-drug solutions were stirred for 2 h before addition to HyA solution. After the preparation of drug loaded particles, same purification protocol was used as for the drug-free particles. Drug optimization studies were carried out for BSA-containing samples, and the optimized ratio was used for fabrication of HSA-based formulas because of the similar structure and same IBU binding capability of the proteins.

2.4. Methods

2.4.1. Particle charge detector (PCD)

A PCD-04 Particle Charge Detector [22,29] (Mütek Analytic GmbH, Germany) was used to determine quantitatively the different charge neutralization point of the proteins at pH = 6.5, where the permeability and drug dissolution studies have been carried out. The BSA and HSA aqueous solutions (c = 0.36 mg mL^{-1}, 20.0 mL, pH = 6.5) were titrated with CTAB solution (c = 10.0 mM); in every step 10–20 μL portions to the CTAB solution were added to the protein-containing samples at 25 °C and the streaming potential values (mV) were registered as a function of CTAB amount.[1] The regular sigmoidal character of charge titration curves is strongly distorted, a modified version of the sigmoidal Boltzmann equation [30] was used to fit the experimental data. The steps of the calculations were summarized in the Suppl. Inf with the equation.

2.4.2. Circular dichroism spectroscopy

CD spectra were recorded in the middle – UV region 200–300 nm using a Jasco J-1100CD spectrometer. The CD spectra recorded by using 1 cm optical path length quartz cuvette at 25 and 37 ± 1 ℃ under N_2 flow (3 L min^{-1}) and each spectrum represents the average of three scans registered at 100 nm min^{-1} scanning speed. The light source was a water-cooled, high-energy xenon lamp (450 W). For evaluation of the secondary structure of proteins, the SpectraManager software was used, and the CD curves are fitted by Yang-model [31,32]. For each measurement, the registered primer spectrum is corrected with the buffer/drug/HyA solution (in the same concentration than in the presence of serum albumin). The raw data was converted into mean residue

[1] For pure proteins, the streaming potential values were measured as a function of pH. The experimental conditions of these titrations were presented in [15].

ellipticity (MRE) using Eq. (1), and the ratio of the α-helix content was calculated from the Eq. (2) [31].

$$MRE_{208} = \frac{observedCD(mdeg)}{10C_p nl} \quad (1)$$

$$\alpha - helix(\%) = \frac{-MRE_{208} - 4000}{33000 - 4000} \times 100 \quad (2)$$

where the C_p is the molar concentration of the protein, n is the number of amino acid residues, and l is the pathlength of the cuvette. The measurements were repeated two times.

2.4.3. Characterization of the prepared drug-carrier particles

Average size, size distribution, polydispersity index (PDI) and Zeta-potential (ζ-potential) values were measured by DLS using a HORIBA SZ-100 NanoParticle Analyzer (Retsch Technology GmbH, Germany). For every sample, the measurements were repeated three times, and for each sample 10 parallel data points were recorded. The light source was a semiconductor laser (λ = 532 nm, 10 mW) and photomultiplier tubes (PMT) were used as detector at 90° scattering angle. For TEM studies a Jeol JEM-1400plus equipment (Japan) at 120 keV accelerating voltage was applied. Turbidity measurements were performed by a Precision Bench Turbidity MeterLP2000 equipment in the range of 50 – 1000 FTU (FTU = Formazin Turbidity Unit, Hanna Inst, Szeged, Hungary). The absorbance spectra of the proteins were recorded on Shimadzu UV-1800 UV Spectrophotometer using 1 cm quartz cuvette in the range of 200–500 nm. The pH measurements were carried out on a Mettler Toledo SevenEasy pH meter equipped with a combined glass pH-electrode (filled with 3.5 M KCl, HI1131, Hanna Instr., Szeged, Hungary). The system was calibrated before measurements.

2.4.4. In vitro dissolution studies and determination of IBU-albumin binding

To investigate the *in vitro* dissolution kinetics and release profile of IBU containing carriers at intestinal conditions, the Rapid Equilibrium Dialysis (RED) device (Thermo Scientific™, Waltham, MA, USA) was used. A solution of IBU was prepared in PBS (pH = 6.5) with the nominal concentration of 0.1 mg mL^{-1} as a control, while 1.0 mg of both formulas (BSA- or HSA-based) were redispersed in 1.0 mL PBS (pH = 6.5) for each measurement. Both the control and the formulas were homogenized using an Eppendorf MixMate (Thermo Scientific™, Waltham, MA, USA) vortex mixer for 30 s and an ultrasonic bath (Sonorex Digiplus, Bandelin GmbH & Co. KG, Berlin, Germany) for 10 min. The RED Device inserts (8 K MWCO) were fitted into the PTFE base plate, then 150 μL of samples was placed into the donor chambers, while 300 μL of PBS (pH = 6.5) was added to the acceptor chambers. Thereafter the RED unit was covered with a sealing tape and incubated at 37 °C on an orbital shaker (at 350 rpm) for 6 h. 50 μL aliquots were withdrawn from the acceptor chamber at 5, 15, 30, 60, 120, 240 and 360 min time points and immediately replaced with the same amount of fresh medium. 50 μL of MeCN was added to the withdrawn samples and the IBU content was determined using HPLC-DAD. Five parallel measurements were performed. For determination of IBU-HSA/BSA binding RED Device inserts (8 K MWCO) were fitted into the reusable Teflon base plate, then 200 μL of samples were placed into the donor chamber (indicated by the coloured retainer ring). Sample solutions were prepared at 20 μM initial concentration (0.1 % DMSO; 0.9 % MeCN) by adding 30 μL of 10 mM DMSO stock solutions to 270 μL MeCN, producing a 1 mM solution, then adding 10 μL of the 1 mM solution to 990 μL of HSA/BSA solution (4 g L^{-1} HSA/BSA in PBS, pH = 7.4). Then 350 μLs of dialysis buffer (PBS, pH = 7.4) were added to the buffer chambers, the unit was covered with sealing tape and incubated at 37 °C on an orbital shaker (at 350 rpm) for 4.5 h. After incubation, the seal was removed and 100 μL aliquots of post-dialysis samples from the donor and buffer chambers were withdrawn. Then 300 μL of precipitation buffer (cold acetonitrile/water (90:10 v/v%), containing 0.1 % formic acid) were added to each sample to precipitate the protein and release IBU. The samples were vortexed and incubated on ice for 30 min, then centrifuged for 10 min at 14000 × g. After centrifugation, the supernatants (200 μL) were transferred to vials for HPLC-DAD analysis to determine IBU concentration in the donor and buffer chambers. Five parallel measurements were performed. The percentage of the test compound bound was calculated using Eq. (3):

$$Binding(\%) = \left(1 - \frac{c_b}{c_d}\right) \cdot 100 \quad (3)$$

where c_b and c_d are the concentrations of the test compound in the buffer and donor chamber, respectively. The significance of differences of dissolution data was calculated with one-way ANOVA with post hoc test (Tukey's multiple comparisons test, α = 0.05).

2.4.5. Permeability studies

'In house developed' and earlier published [33] intestinal parallel artificial membrane permeability assay (intestinal (I)-PAMPA) system was applied to determine effective I-specific permeability of IBU from reference solution and formulas in comparison study. The same donor solutions (pH = 6.5) were used as in the case of dissolution studies. The filter donor plate (Multiscreen™-IP, MAIPN4510, pore size 0.45 μm; Millipore) was coated with 5 μL of lipid solution (16 mg PC + 8 mg CHO dissolved in 600 μL dodecane). Then the donor plate was fit into the acceptor plate (Multiscreen Acceptor Plate, MSSACCEPTOR; Millipore) containing 300 μL of PBS solution (pH = 7.4), and 150 μL of the donor solutions were put on the membrane of the donor plate. The donor plate was covered with a sheet of wet tissue paper and a plate lid to avoid evaporation of the solvent. The sandwich system was incubated at 37 °C for 4 h (Heidolph Titramax 1000), followed by separation of the PAMPA sandwich plates and the determination of concentrations of IBU in the acceptor solutions by HPLC-DAD in six parallel measurements. The effective permeability and membrane retention of drugs were calculated using Eq. (4) [34]:

$$P_e(cm/s) = -\frac{2.303 \cdot V_A}{A(t - \tau_{SS})} \cdot \log[1 - \frac{c_A(t)}{S}] \quad (4)$$

where P_e is the effective permeability coefficient (cm s^{-1}), A is the filter area (0.24 cm^2), V_A is the volume of the acceptor phase (0.3 mL), t is the incubation time (s), τ_{SS} is the time to reach the steady state (s), $c_A(t)$ is the concentration of the compound in the acceptor phase at time point t (mol mL^{-1}), and S (mol mL^{-1}) is the solubility of IBU in the donor phase. The flux of samples was calculated with Eq. (5) [34]:

$$Flux(mol/cm^2 \cdot s) = P_e \cdot S \quad (5)$$

The significance of differences of dissolution data was calculated with one-way ANOVA with post hoc test (Tukey's multiple comparisons test, α = 0.05).

2.4.6. HPLC method

The determination of IBU concentration was performed with an Agilent 1260 HPLC (Agilent Technologies, Santa Clara, USA). A Kinetex® EVO C18 column (5 μm, 150 mm × 4.6 mm (Phenomenex, Torrance, CA, USA)) was used as stationary phase. The mobile phases consisted of purified water adjusted to pH = 3.0 with phosphoric acid (A), and acetonitrile (B). An isocratic elution was performed for 5 min with 60–40 % A-B eluent composition. Separation was performed at 25 °C with 1 mL min^{-1} flow rate.

10 μL of the samples was injected to determine the IBU concentration at 220 nm using UV–VIS diode array detector. Data were evaluated using ChemStation B.04.03. Software (Agilent Technologies, Santa Clara, USA). The retention time of IBU was observed at 3.61 min. The regression coefficient (R2) of the calibration curve was 0.999 in the concentration range 5–500 μg mL^{-1}. The determined limits of detection (LOD) and quantification (LOQ) of IBU were 6 ppm and 18 ppm, respectively.

3. Results and discussion

3.1. Determination of the maximum encapsulable IBU content by CD

In the first part of this article [15] m_{IBU}/m_{BSA} = 0.25 ratio was used to confirm the applicability of serum albumin/polysaccharide complex carrier on IBU encapsulation by several spectroscopic and thermoanalytical techniques. The preparation possibilities of albumin/HyA complex carriers in the presence of increased IBU content are investigated in detail. During preparation the first decisive step is the formation of protein-drug complex in aqueous solution. To optimize the maximum amount of IBU to be added to protein (in the absence of HyA), changes in BSA structure were monitored upon administration of IBU to BSA by CD studies. CD curves of BSA were registered in the absence and in the presence of IBU at various ratios (m_{IBU}/m_{BSA} = 0.25; 1; 2; 4). Similar experiments were carried out for HSA as well, while the albumin concentrations are remained the same (c = 0.027 mg mL^{-1}). The registered CD curves for BSA-containing systems are shown in Fig. 1**.** The characteristic negative bands of pure BSA appear at 208 and 220 nm. By increasing drug amount, the intensity of the negative band at 208 nm is changed proportionately [35]. At m_{IBU}:m_{BSA} = 4.0 the negative band entirely disappears, correlated with the decrease of α-helix content of the protein to nearly zero. Same trends are observed for both serum albumins; the changes in the secondary structural elements are presented in **Table S1**. By the addition of IBU, the α-helix content is decreased proportionally with the increase in β-sheet and random conformation contents. The values of α-helix contents for each sample are also verified using Eq. (2).

CD measurements confirmed that a significant decrease in α-helix content occurs with increasing serum protein and drug mass ratio, and accordingly the amount of IBU to be encapsulated can be maximized. In the presence of larger quantity of IBU (m_{IBU}/m_{BSA} > 2.0) the BSA-IBU complexes precipitate, and the formation of further colloidal particles is not suitable. Based on visible changes in the sample (Fig. 2**.A** photos) and the results of CD measurements, the m_{IBU}/m_{BSA} = 2.0 ratio was fixed for preparation of the composites with optimized size and drug content.

3.2. Structural characterization of the IBU-containing colloidal particles

The effect of the enhanced drug amount was investigated on the characteristic features (size, morphology, protein structure, stability) of the complex particles as well by several techniques using m_{IBU}/m_{BSA} = 0.125 – 4.0 mass ratios, where the BSA/HyA 2:1 wt ratio was kept constant. Fig. 2**.A.** clearly represents the change of the average hydrodynamic diameter of the particles (left y-axis) and the turbidity values (right y-axis) at different m_{IBU}/m_{BSA} under the preparation conditions (in acetate buffer, pH = 4.5). The measured values show, that below the m_{IBU}/m_{BSA} = 2.0 ratio the particles remain stable, the size varied between *ca.* 180–260 nm and turbidity is also measurable. If the drug/protein ratio exceeds the 2.0, aggregation of the particles is started (d_{DLS} ∼ 380–400 nm) and even in the short-term study (3–4 min), the particles cannot be considered stable, and the size cannot be measured by DLS.

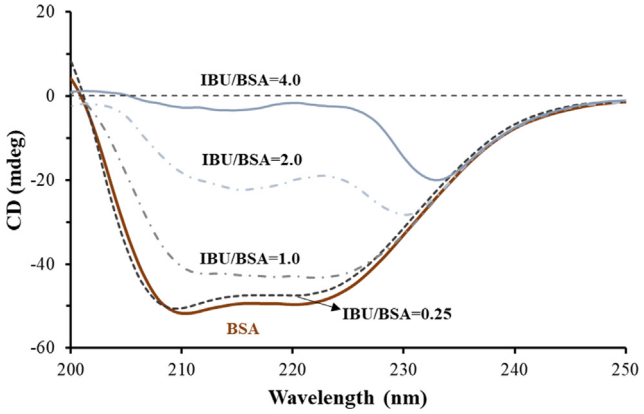

Fig. 1. The measured CD spectra of BSA without and with IBU at different m_{IBU}/m_{BSA} = 0.25; 1.0; 2.0; 4.0 ratios (c_{BSA} = 0.027 mg mL^{-1}, acetate buffer pH = 4.5).

Because of the precipitation (as the inserted photo of the sample shows) the turbidity is reduced to zero.

The measured ζ-potential values also support this observation, because above the mass ratio of 2.0 the nearly – 40 mV decreases to almost 0 mV. Changes in polydispersity index (PDI) recorded by DLS measurements are also in good agreement with these findings. The ζ-potential and PDI values are shown in **Figure S1**. The DLS and turbidity results clearly correlate with the main findings of CD studies, thus the amount of encapsulating IBU can be maximized. According to the TEM images (Fig. 2**.B**), it can be concluded that nearly spherical morphology is dominant and increase in the drug amount results in the slightly increase in the size of the drug-loaded formulas. At higher drug content (m_{IBU}/m_{BSA} > 2.0), in agreement with the results of DLS and turbidity, aggregation of the particles occurs. Based on the above-mentioned conclusions of four different techniques, the $m_{IBU}/m_{BSA}/m_{HyA}$ = 2:1:0.5 ratio was used to prepare drug-loaded particles for PAMPA permeability tests. Because of the nearly same structure of BSA and HSA and the similar IBU binding capability (BSA-IBU: $\log K_{b1}$ = 5.90; HSA-IBU: $\log K_{b1}$ = 5.95 determined by ITC [36] for 1:1 stoichiometry processes) this optimized drug/protein/polysaccharide ratio was applied for fabrication of HSA-based particles, as a new formula. Fig. 3. shows a representative size distribution curve registered by DLS and a TEM image of HSA-based particles using $m_{IBU}/m_{HSA}/m_{HyA}$ = 2:1:0.5 wt ratio. Nearly same particle sizes are detected, but a more characteristic spherical morphology is observed for HSA-based systems. For both formulas, the combination of BSA or HSA with HyA, results in *ca.* 30 % of drug loading. Based on this high DL%, presumably the IBU is located not only in the binding sites of the proteins, but also fixed by outer polysaccharide matrix and the extra hydrophilic character of HyA may also increase in the equilibrium solubility of IBU.

Before *in vitro* permeability measurements, the characteristic features (size, stability) of the redispersed formulas were investigated. The representative size distribution curves in **Figure S2** clearly demonstrate that the size does not change measurable after 3 months redispersed the particles in acetate buffer (pH = 4.5) due to the presence of the electrostatic interactions between the macromolecules. Namely, at pH = 4.5 the total charge of the protein is more positive (pI_{BSA} ∼ 5.1; pI_{HSA} ∼ 4.6), which is clearly seen on Fig. 4. Fig. 4. shows the change of the streaming potential values of BSA and HSA as a function of pH, the isoelectric point (pI) is detected, when the streaming potential values reach the zero mV.

The change of the streaming potential values for HyA solution have also been registered as a function of pH, the results were presented in the first part of this work (Ref. [15], Fig. 2). It can be stated that the HyA is fully deprotonated above pH = 4 [15]. For HyA

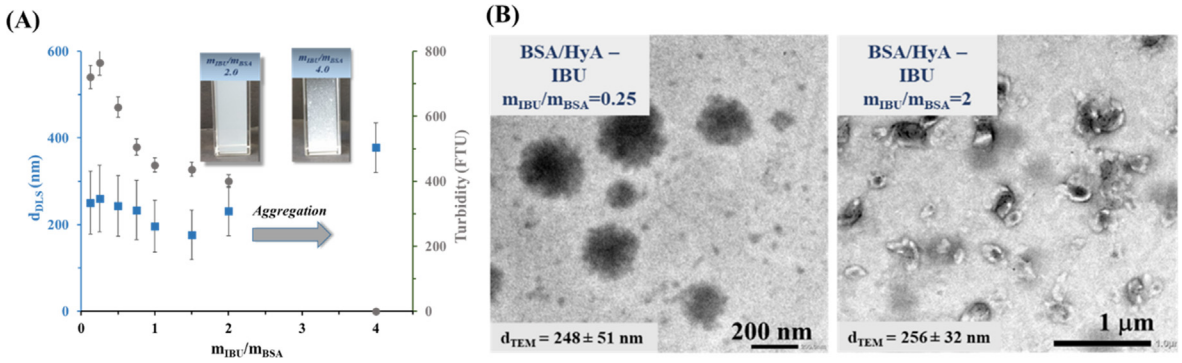

Fig. 2. Change of the hydrodynamic diameters (marked with square, left y-axis) and turbidity values (marked with circle, right y-axis) of IBU-containing BSA-based formulas at pH = 4.5 using various IBU content (m_{BSA} = 4.0 mg, t = 25 °C) **(A)** and representative TEM images of the BSA/HyA – IBU particles at two different drug/protein ratios with the calculated average diameters **(B)**.

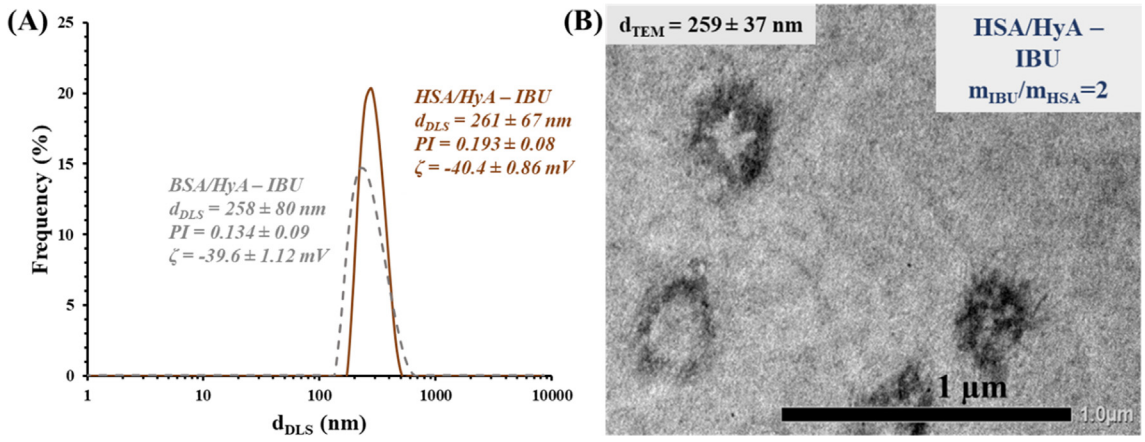

Fig. 3. Size distribution curves of the BSA-(dotted line) and HSA/HyA – IBU particles (continuous line) at $m_{IBU}/m_{protein}/m_{HyA}$ = 2:1:0.5 wt ratio (**A**) and a TEM image of HSA-based particles with the calculated average diameter (**B**).

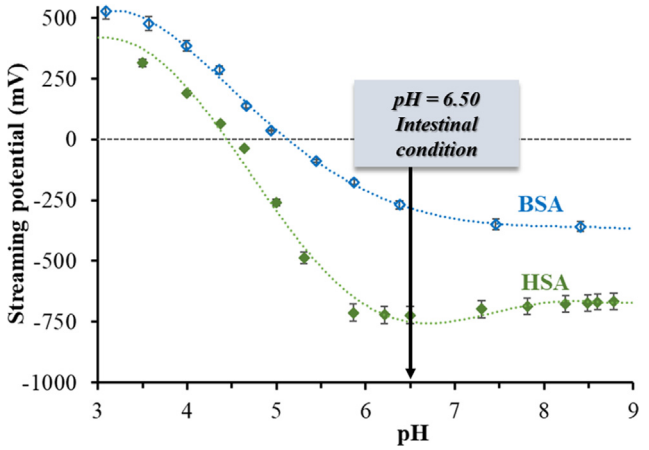

Fig. 4. Charge titration curves of the proteins as a function of pH ($c_{protein}$ = 0.36 mg mL^{-1}).

we cannot give only one value for pK_a, a smaller interval can be specified only, which is 3–4 [37]. As we mentioned in the Introduction, the pK_a of the IBU is 4.4 – 4.9 (depending on the ionic strength, medium and techniques) [22], so the ratio of the protonated and deprotonated forms is *ca.* 50–50% at pH = 4.5, but in case of the binding of IBU to the serum proteins the charge is not the determining factor. Moreover, we intent to examine the stability as well as the structure of the drug-loaded BSA- and HSA/HyA formulas at pH = 6.5 as well where the permeability studies have been carried out. Based on the above-mentioned acid-base properties of the components, we can conclude that both the macromolecules (albumins and HyA) and the IBU is fully deprotonated and have a negative charge at this pH. The prepared formulas were redispersed in PBS (pH = 6.5), and after 30 min the size of the particles was measured by DLS (Fig. 5**.A**).

According to the dynamic light scattering and spectroscopic measurements, most probable the dominantly hydrophilic HyA starts to detach from the outer shell and form a loose skein (d ~ 740 nm) and an inner core (d_{core} ~ 90 nm) is remained containing mostly the protein/drug complex. The DLS studies were followed by CD as well. The registered CD curves of the HSA (Fig. 5**.B**), corrected for the presence of components[2], show measurable differences at pH = 4.5 and at pH 6.5 compared to pure protein. The α-helix content decreases from *ca.* 50 % to 10–11% due to the formation of composite particles at pH = 4.5. Moreover, at pH = 6.5 the α-helix content continues to decrease further by approx. 2–3 %. This dominant structural change clearly confirms the DLS results. Below the isoelectric point of the protein (the net charge of the albumin is positive) the formula remains stable, but if the pH of the media is above the isoelectric point (the net charge of the albumin becomes negative) the electrostatic interaction disappears, and the composite gradually disintegrates and the IBU molecules start to release from

[2] The primer CD curves of HSA (same CD curve can be registered for BSA as well) and the HyA are presented in **Figure S3.**

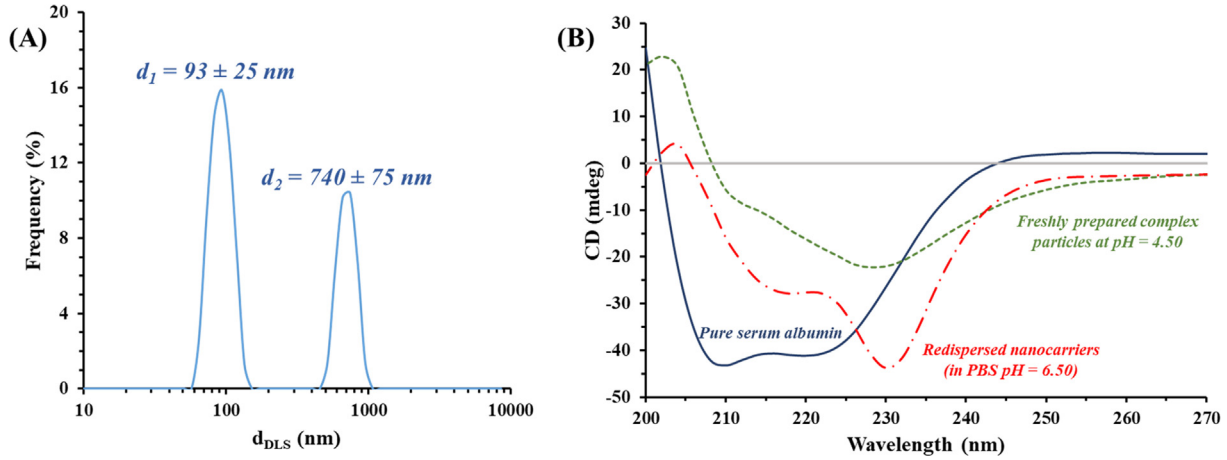

Fig. 5. DLS curve of the aqueous dispersion containing HSA/HyA – IBU particles at pH = 6.5 (**A**) and the CD curves of the HSA in pure form and in the formulas at pH = 4.5 and 6.5. (**B**) (c_{HSA} = 0.0027 mg mL^{-1}).

the formulation. The release of the active drug from the composite may partially induced by these structural changes of the serum protein. This mechanism is also supported by UV–Vis (**Figure S4**). The UV–Vis spectra of the composite dispersion were registered as a function of the time after dispersion the samples in PBS buffer. The absorbance of the characteristic band of BSA and HSA at 280 nm showed a gradually increasing trend, suggesting detachment of the outer HyA shell and gradual appearance of protein in the inner core. The change of the pH of the dispersions were followed as a function of the time, but no measurable changes were detected (**Figure S5**).

3.3. In vitro drug release and determination of albumin binding of IBU

Drug release kinetic of each formula is a critical part of formulation design as it is the major determining factor on the drug delivery of the carrier *in vivo* and the subsequent release of the free drug. The *in vitro* release profile reveals important information from the structure and behaviour of the formulas, especially the electrostatic interactions between the drug and carrier system and a kinetic effect, and their influence on the rate and mechanism of drug release. In the RED system, IBU containing carriers are physically separated from the acceptor media by an 8 kDa MWCO dialysis membrane, which allows only the passive diffusion of unbound IBU released from carrier into the acceptor media. The time-dependent *in vitro* release profiles of IBU containing formulas and its unformulated form (IBU) (Fig. 6.) were investigated at intestinal conditions (pH = 6.5). Due to the weak acidic character of IBU (pK_a = 4.59 [34]) it can be found in fully ionized form in dissolution medium (2 < ΔpH=|pH-pK_a|), although the dissolution profile of IBU shows only a slight increase, after 120 min the equilibrium solubility (256 ± 9 μM) was reached. In case of formulations, a significantly increased dissolution was observed compared to IBU (**, p < 0.01), which can be claimed with the nano size, increased specific surface area and negative surface charge of albumin/HyA-IBU formulas.

The dissolution profiles of HSA- and BSA-based formulations clearly demonstrate the effect of protein-binding on the drug release. The lower protein binding of HSA resulted in higher repulsion between negatively charged HSA/HyA and IBU, therefore significantly higher drug release (**, p < 0.01) in sampling intervals compared to BSA/HyA-IBU. Our results showed the protein-binding of HSA-IBU was 52 ± 3.97%, whereas of BSA-IBU 85 ± 3.33%, which supports with the drug release study. The apparent increase in the solubility and the release of the encapsulated IBU are driven partially by the interactions between the IBU and the carrier. Besides that, the apparent increase of the solubility of IBU formulated into the carrier system can also be a kinetic effect that is only indirectly related to the interaction of IBU with the carrier. The fast dissolution of IBU takes place in pseudo-equilibrium starting from its molecularly dispersed (amorphous) form in the nanosized carrier, which gives a supersaturated solution with respect to crystalline IBU. Crystalline IBU can only slowly precipitate from this supersaturated solution and establish the thermodynamic solubility equilibrium between crystalline and dissolved IBU. The main effects resulting in the temporal apparent solubility increase are the following. i) The carrier needs to keep IBU molecularly dispersed (amorphous), and ii) the release of IBU molecules must be fast from the carrier. Importantly, the latter point is governed by the interactions between IBU and the carrier. **Figure S6** presents the drug release curves in other representation mode (c/c_0 vs. t). This representation also confirms that 68% of the loaded IBU is released after 240 min for BSA-based particles, while this value is ~ 81 % for HSA-based carriers. These release curves were fitted by the Weibull-model [15], which provided the best fit of the primer data. The fitted curves are presented in **Fig. S7**.

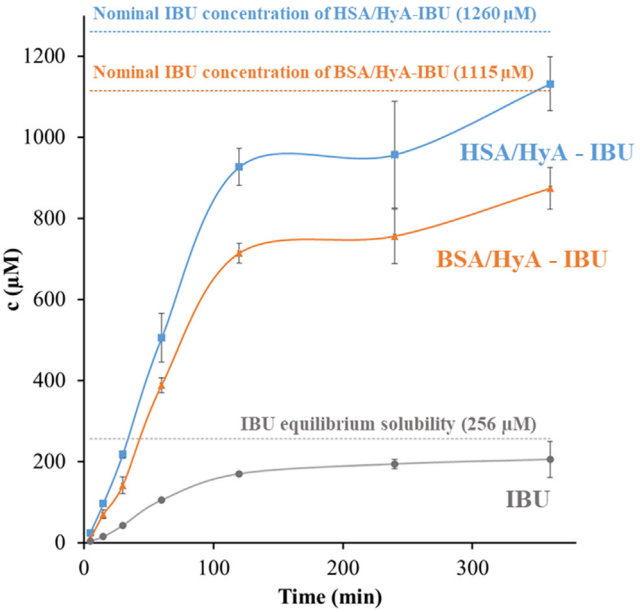

Fig. 6. *In vitro* drug release of IBU containing formulas in comparison to unformulated IBU. Data is presented as means ± SD, n = 5.

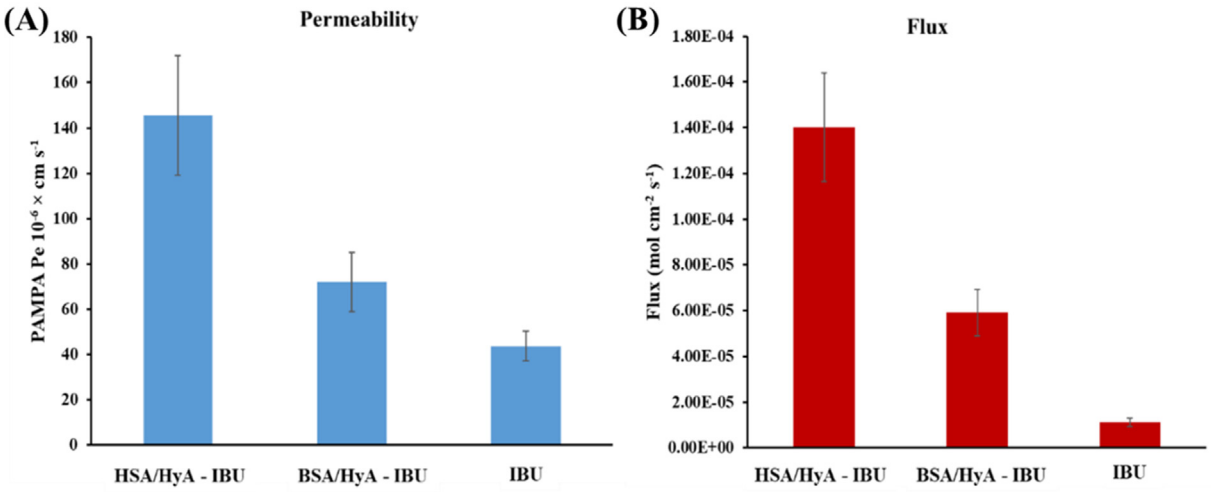

Fig. 7. Intestinal-specific permeability **(A)** and flux (**B**) of IBU-loaded carriers in comparison to unformulated IBU. Data is presented as means ± SD, n = 6.

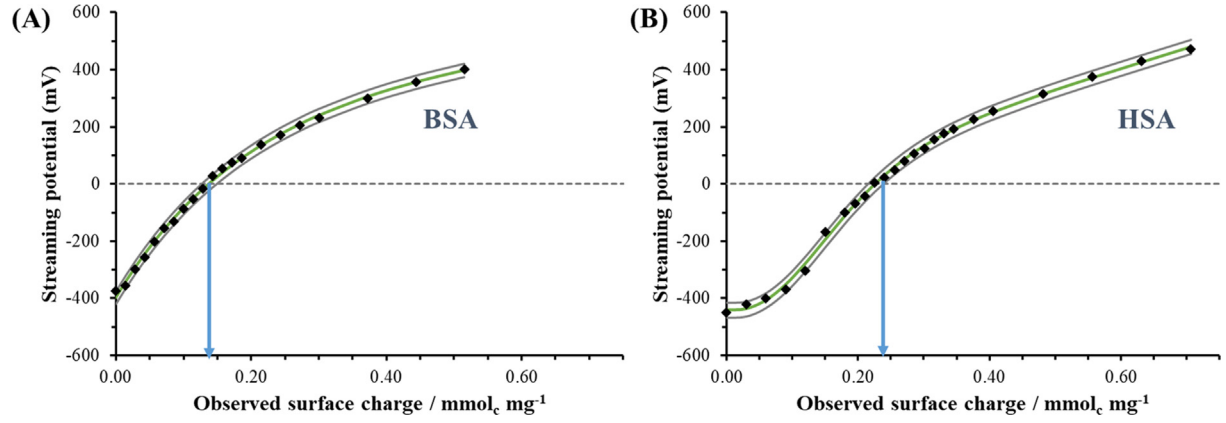

Fig. 8. Charge titration curves of (**A**) BSA and (**B**) HSA as a function of observed surface charge titrated the proteins with CTAB at pH = 6.50 ($c_{protein}$ = 0.36 mg mL^{-1}, $V_{protein}$ = 20.0 mL; c_{CTAB} = 10.0 mM, V_{CTAB} = 10–20 μL/per titration points) (The continuous grey lines represent the confidential intervals of the measured points).

3.4. Intestinal-specific permeability study

Fig. 7. shows the intestinal permeability of two formulas in comparison to starting IBU in intestinal-PAMPA system. Both carriers significantly increased the permeability and flux of IBU compared to unformulated IBU (HSA/HyA-IBU vs. IBU ***, $p < 0.001$; BSA/HyA-IBU vs. IBU ***, $p < 0.001$). The increased permeability and flux of IBU revealed for investigating the formulas can be explained by the solubilizing effect of HSA and BSA. Comparing the permeability and flux of formulas significant difference was observed (***, $p < 0.001$) in both cases, which corresponds to drug release study results. Both permeability and flux results support both formulas can facilitate passive transport of IBU, which is an important parameter by the intestinal absorption.

3.5. Quantification of the protein charges at intestinal condition (pH = 6.5)

The *in vitro* dissolution and permeability studies confirm that there are differences between BSA- and HSA-based formulas which may result from the variant protonation states of the proteins and differences in surface charge at pH = 6.5. To confirm these findings, quantitative particle charge titrations were carried out. Fig. 4. clearly shows the change of the streaming potential values of BSA and HSA as a function of pH. The streaming potential values show measurable difference at pH = 6.50 (BSA ∼ − 310 mV, HSA ∼ -725 mV) which indicate different charge states of the proteins at this pH. To quantify these differences, the proteins were titrated at pH = 6.50 with CTAB surfactant having one positive charge/molecule. As Fig. 8**.** presents, for BSA (Fig. 8.**A**) less positively charged CTAB (q = 0.131 ± 0.024 mmol mg^{-1}) is necessary to reach the charge compensation point than for HSA (q = 0.226 ± 0.012 mmol mg^{-1}) under same protein concentration. These quantitative results clearly support, that the BSA contains less negative charge (q = 0.131 ± 0.024 mmol mg^{-1}) than the HSA (q = 0.226 ± 0.012 mmol mg^{-1}) under same pH conditions and thus the repulsive interactions between HSA and the negatively charges IBU drug molecules are stronger. Based on this conclusion, the larger drug retention as well as the more significant permeability and flux were quantitatively confirmed.

4. Conclusion

The successful applicability of a biodegradable serum albumin-HyA complex carrier particles for IBU encapsulation with the maximized 30% of drug loading was demonstrated. As expected, these formulations have more favourable dissolution and intestinal permeability and flux properties than unformulated IBU.

In connection with the physicochemical characterization of HSA / BSA formulations, due to the increased negative charge of HSA, the accelerated dissolution and increased permeability / flux of ionized IBU (pH 6.5, pK_a = 4.59) for HSA/HyA-IBU was achieved compared to BSA/HyA-IBU in the simulated intestinal medium. The nanosized carrier formula, which provides increased solubility, accelerated dissolution, and greater permeability, may represent a more controlled, lower dose loading, and gastric mucosa-sparing therapeutic solution in the human therapeutic use of ibuprofen. The application of intestinisolvent-gastroresistant capsules as carrier can be a suitable tool for protecting albumin/HyA formulations against acidic condition and enzymatic digestion of stomach. This approach can effectively support the targeted liberation of drug at the site of absorption.

Declaration of Competing Interest

The authors declare that they have no known competing financial interests or personal relationships that could have appeared to influence the work reported in this paper.

Acknowledgement

Project no. TKP2021-EGA-32 has been implemented with the support provided by the Ministry of Innvation and Technology of Hungary from the National Research, Development and Innovation Fund, financed under the TKP2021-EGA-32 funding scheme. This research was also supported by the NRDIH through FK131446 project. The publication was also funded by the University of Szeged Open Access Fund (FundRef, Grant No. 5598). Á. Juhász thanks the financial support of the ÚNKP-21-4-SZTE-516 new National Excellence Program of the Ministry for Innovation and Technology from the source of the NRDIF and the János Bolyai Research Fellowship of the Hungarian Academy of Sciences (Á. Juhász)

Appendix A. Supplementary material

Supplementary data to this article can be found online at https://doi.org/10.1016/j.molliq.2022.118614.

References

[1] M. Karimi, S. Bahrami, S.B. Ravari, P.S. Zangabad, H. Mirshekari, M. Bozorgomid, S. Shahreza, M. Sori, M.R. Hamblin, Albumin nanostructures as advanced drug delivery systems, Expert Opin. Drug Deliv. 13 (11) (2016) 1609–1623, https://doi.org/10.1080/17425247.2016.1193149.

[2] G. Huerta-ángeles, K. Nešporová, G. Ambrožová, L. Kubala, V. Velebný, An effective translation: The development of hyaluronan-based medical products from the physicochemical, and preclinical aspects, Front. Bioeng. Biotechnol. 6 (2018) 62, https://doi.org/10.3389/fbioe.2018.00062.

[3] F. Bai, Y. Wang, Q. Han, M. Wu, Q. Luo, H. Zhang, Y. Wang, Cross-linking of hyaluronic acid by curcumin analogue to construct nanomicelles for delivering anticancer drug, J. Mol. Liq. 288 (2019) 111079, https://doi.org/10.1016/j.molliq.2019.111079.

[4] A. Aguilera-Garrido, J.A. Molina-Bolívar, M.J. Gálvez-Ruiz, F. Galisteo-González, Mucoadhesive properties of liquid lipid nanocapsules enhanced by hyaluronic acid, J. Mol. Liq. 296 (2019) 111965, https://doi.org/10.1016/j.molliq.2019.111965.

[5] E. Larrañeta, M. Henry, N.J. Irwin, J. Trotter, A.A. Perminova, R.F. Donnelly, Synthesis and characterization of hyaluronic acid hydrogels crosslinked using a solvent-free process for potential biomedical applications, Carbohydr. Polym. 181 (2018) 1194–1205, https://doi.org/10.1016/j.carbpol.2017.12.015.

[6] A. Dag, Y. Jiang, K.J.A. Karim, G. Hart-Smith, W. Scarano, M.H. Stenzel, Polymer-albumin conjugate for the facilitated delivery of macromolecular platinum drugs, Macromol. Rapid Commun. 36 (10) (2015) 890–897, https://doi.org/10.1002/marc.201400576.

[7] E. Csapó, Á. Juhász, N. Varga, D. Sebők, V. Hornok, L. Janovák, I. Dékány, Thermodynamic and kinetic characterization of pH-dependent interactions between bovine serum albumin and ibuprofen in 2D and 3D systems, Colloids Surfaces A Physicochem. Eng. Asp. 504 (2016) 471–478.

[8] V. Hornok, Á. Juhász, G. Paragi, A.N. Kovács, E. Csapó, Thermodynamic and kinetic insights into the interaction of kynurenic acid with human serum albumin: Spectroscopic and calorimetric approaches, J. Mol. Liq. 313 (2020) 112869, https://doi.org/10.1016/j.molliq.2020.112869.

[9] M. Fasano, S. Curry, E. Terreno, M. Galliano, G. Fanali, P. Narciso, S. Notari, P. Ascenzi, The extraordinary ligand binding properties of human serum albumin, IUBMB Life 57 (12) (2005) 787–796, https://doi.org/10.1080/15216540500404093.

[10] F. Yang, Y. Zhang, H. Liang, Interactive association of drugs binding to human serum albumin, Int. J. Mol. Sci. 15 (2014) 3580–3595, https://doi.org/10.3390/ijms15033580.

[11] M.L. Verma, B.S. Dhanya, Sukriti, V. Rani, M. Thakur, J. Jeslin, R. Kushwaha, Carbohydrate and protein based biopolymeric nanoparticles: Current status and biotechnological applications, Int. J. Biol. Macromol. 154 (2020) 390–412, https://doi.org/10.1016/j.ijbiomac.2020.03.105.

[12] D. Ding, X. Jiang, Drug Delivery from Protein-Based Nanoparticles, Bioinspired Biomim, Polym. Syst. Drug Gene Deliv. 9783527334 (2015) 149–170, https://doi.org/10.1002/9783527672752.ch6.

[13] S.M.H. Hosseini, Z. Emam-Djomeh, P. Sabatino, P. Van der Meeren, Nanocomplexes arising from protein-polysaccharide electrostatic interaction as a promising carrier for nutraceutical compounds, Food Hydrocoll. 50 (2015) 16–26, https://doi.org/10.1016/j.foodhyd.2015.04.006.

[14] M. Mendes, T. Cova, J. Basso, M.L. Ramos, R. Vitorino, J. Sousa, A. Pais, C. Vitorino, Hierarchical design of hyaluronic acid-peptide constructs for glioblastoma targeting: Combining insights from NMR and molecular dynamics simulations, J. Mol. Liq. 315 (2020) 113774, https://doi.org/10.1016/j.molliq.2020.113774.

[15] A.N. Kovács, N. Varga, Á. Juhász, E. Csapó, Serum protein-hyaluronic acid complex nanocarriers: Structural characterisation and encapsulation possibilities, Carbohydr. Polym. 251 (2021) 117047, https://doi.org/10.1016/j.carbpol.2020.117047.

[16] E. Csapó, H. Szokolai, Á. Juhász, N. Varga, L. Janovák, I. Dékány, Cross-linked and hydrophobized hyaluronic acid-based controlled drug release systems, Carbohydr. Polym. 195 (2018) 99–106, https://doi.org/10.1016/j.carbpol.2018.04.073.

[17] L.J. Crofford, Use of NSAIDs in treating patients with arthritis, Arthritis Res. Ther. 15 (2013) 1–10, https://doi.org/10.1186/ar4174.

[18] L. Aabakken, Small-bowel side-effects of non-steroidal anti-inflammatory drugs, Eur. J. Gastroenterol. Hepatol. 11 (4) (1999) 383–388, https://doi.org/10.1097/00042737-199904000-00004.

[19] C. Patrono, C. Baigent, Nonsteroidal anti-inflammatory drugs and the heart, Circulation 129 (8) (2014) 907–916, https://doi.org/10.1161/CIRCULATIONAHA.113.004480.

[20] W. Badri, K. Miladi, Q.A. Nazari, H. Greige-Gerges, H. Fessi, A. Elaissari, Encapsulation of NSAIDs for inflammation management: Overview, progress, challenges and prospects, Int. J. Pharm. 515 (1-2) (2016) 757–773, https://doi.org/10.1016/j.ijpharm.2016.11.002.

[21] C. Sostres, C.J. Gargallo, M.T. Arroyo, A. Lanas, Adverse effects of non-steroidal anti-inflammatory drugs (NSAIDs, aspirin and coxibs) on upper gastrointestinal tract, Best Pract. Res. Clin. Gastroenterol. 24 (2) (2010) 121–132, https://doi.org/10.1016/j.bpg.2009.11.005.

[22] S. Babić, A.J.M. Horvat, D. Mutavdžić Pavlović, M. Kaštelan-Macan, Determination of pKa values of active pharmaceutical ingredients, TrAC -, Trends Anal. Chem. 26 (11) (2007) 1043–1061, https://doi.org/10.1016/j.trac.2007.09.004.

[23] M. Newa, K.H. Bhandari, D.H. Oh, Y.R. Kim, J.H. Sung, J.O. Kim, J.S. Woo, H.G. Choi, C.S. Yong, Enhanced dissolution of ibuprofen using solid dispersion with poloxamer 407, Arch. Pharm. Res. 31 (11) (2008) 1497–1507, https://doi.org/10.1007/s12272-001-2136-8.

[24] M. Newa, K.H. Bhandari, D.X. Lee, J.H. Sung, J.A. Kim, B.K. Yoo, J.S. Woo, H.G. Choi, C.S. Yong, Enhanced dissolution of ibuprofen using solid dispersion with polyethylene glycol 20000, Drug Dev. Ind. Pharm. 34 (10) (2008) 1013–1021, https://doi.org/10.1080/03639040701744095.

[25] M. Newa, K.H. Bhandari, J.O. Kim, J.S. Im, J.A. Kim, B.K. Yoo, J.S. Woo, H.G. Choi, C.S. Yong, Enhancement of solubility, dissolution and bioavailability of ibuprofen in solid dispersion systems, Chem. Pharm. Bull. 56 (4) (2008) 569–574, https://doi.org/10.1248/cpb.56.569.

[26] KennethC Ofokansi, FranklinC Kenechukwu, RichardO Ezugwu, AnthonyA Attama, Improved dissolution and anti-inflammatory activity of ibuprofen-polyethylene glycol 8000 solid dispersion systems, Int. J. Pharm. Investig. 6 (3) (2016) 139, https://doi.org/10.4103/2230-973X.187344.

[27] M.A. Anaya Castro, I. Alric, F. Brouillet, J. Peydecastaing, S.G. Fullana, V. Durrieu, Soy Protein Microparticles for Enhanced Oral Ibuprofen Delivery: Preparation, Characterization, and In Vitro Release Evaluation, AAPS PharmSciTech. 19 (3) (2018) 1124–1132, https://doi.org/10.1208/s12249-017-0928-5.

[28] L. Hashem, M. Swedrowska, D. Vllasaliu, Intestinal uptake and transport of albumin nanoparticles: Potential for oral delivery, Nanomedicine. 13 (11) (2018) 1255–1265, https://doi.org/10.2217/nnm-2018-0029.

[29] E.S. Dragan, F. Bucatariu, Cross-linked multilayers of poly(vinyl amine) as a single component and their interaction with proteins, Macromol. Rapid Commun. 31 (3) (2010) 317–322, https://doi.org/10.1002/marc.200900630.

[30] Á. Turcsányi, N. Varga, E. Csapó, Chitosan-modified hyaluronic acid-based nanosized drug carriers, Int. J. Biol. Macromol. 148 (2020) 218–225, https://doi.org/10.1016/j.ijbiomac.2020.01.118.

[31] D.M. Rogers, S.B. Jasim, N.T. Dyer, F. Auvray, M. Réfrégiers, J.D. Hirst, Electronic Circular Dichroism Spectroscopy of Proteins, Chem. 5 (11) (2019) 2751–2774, https://doi.org/10.1016/j.chempr.2019.07.008.
[32] W.R. Mason, A Practical Guide to Magnetic Circular Dichroism Spectroscopy, A Pract, Guid. to Magn. Circ. Dichroism Spectrosc. (2006) 1–223, https://doi.org/10.1002/9780470139233.
[33] B. Pethő, M. Zwillinger, J.T. Csenki, A.E. Káncz, B. Krámos, J. Müller, G.T. Balogh, Z. Novák, Palladium-Catalyzed 2,2,2-Trifluoroethoxylation of Aromatic and Heteroaromatic Chlorides Utilizing Borate Salt and the Synthesis of a Trifluoro Analogue of Sildenafil, Chem. - A Eur. J. 23 (62) (2017) 15628–15632, https://doi.org/10.1002/chem.201704205.
[34] A. Avdeef, Absorption and Drug Development: Solubility, Permeability, and Charge State, Absorpt, Drug Dev. Solubility, Permeability, Charg. State. (2012) 698, https://doi.org/10.1002/9781118286067.
[35] F. Mohammadi, A.-K. Bordbar, A. Divsalar, K. Mohammadi, A.A. Saboury, Analysis of binding interaction of curcumin and diacetylcurcumin with human and bovine serum albumin using fluorescence and circular dichroism spectroscopy, Protein J. 28 (3-4) (2009) 189–196, https://doi.org/10.1007/s10930-009-9184-1.
[36] C. Ràfols, S. Zarza, E. Bosch, Molecular interactions between some non-steroidal anti-inflammatory drugs (NSAID's) and bovine (BSA) or human (HSA) serum albumin estimated by means of isothermal titration calorimetry (ITC) and frontal analysis capillary electrophoresis (FA/CE), Talanta 130 (2014) 241–250, https://doi.org/10.1016/j.talanta.2014.06.060.
[37] A. Mero, M. Campisi, Hyaluronic Acid Bioconjugates for the Delivery of Bioactive Molecules, Polymers 6 (2) (2014) 346–369, https://doi.org/10.3390/polym6020346.